Received: 28 June 2019 | Revised: 26 August 2019 | Accepted: 5 September 2019

DOI: 10.1111/cas.14199

ORIGINAL ARTICLE

Cancer Science WILEY

Circulating microRNA-590-5p functions as a liquid biopsy marker in non-small cell lung cancer

Akanksha Khandelwal[1] | Rajeev Kumar Seam[2] | Manish Gupta[2] | Manjit Kaur Rana[3] | Hridayesh Prakash[4] | Karen M. Vasquez[5] | Aklank Jain[6]

[1]Department of Biochemistry and Microbial Sciences, Central University of Punjab, Bathinda, Punjab, India

[2]Department of Radiation Oncology, Indira Gandhi Medical College, Shimla, Himachal Pradesh, India

[3]Department of Pathology, Advanced Cancer Institute, Bathinda, Punjab, India

[4]Institute of Virology and Immunology, Amity University, Noida, Uttar Pradesh, India

[5]Division of Pharmacology and Toxicology, College of Pharmacy, Dell Pediatric Research Institute, The University of Texas at Austin, Austin, TX, USA

[6]Department of Animal Sciences, Central University of Punjab, Bathinda, Punjab, India

Present address
Rajeev Kumar Seam, Department of Radiotherapy, Maharishi Markandeshwar Institute of Medical Sciences and Research, Mullana-Ambala, Haryana, India

Correspondence
Aklank Jain, Department of Animal Sciences, Central University of Punjab, Bathinda, Punjab, India.
Email: aklankjain@gmail.com

Funding information
NIH/NCI, Grant/Award Number: CA093729; Indian Council of Medical Research, Grant/Award Number: 5/13/81/2013-NCD-III

Abstract

Despite the availability of various diagnostic procedures, a tissue biopsy is still indispensable for the routine diagnosis of lung cancer. However, inaccurate diagnoses can occur, leading to inefficient cancer management. In this context, use of circulating microRNAs (miRNAs) may serve as diagnostic tools as liquid biopsies, and as biomarkers to better understand the molecular mechanisms involved in the progression of cancer. We identified miR-590-5p as a potential prognostic marker in the progression of non-small cell lung cancer (NSCLC). We were able to detect this miRNA in blood plasma samples of NSCLC patients through quantitative real-time PCR. Our data showed an ~7.5-fold downregulation of miR-590-5p in NSCLC patients compared to healthy controls, which correlated with several clinicopathological features. Further, overexpression of miR-590-5p led to decreased cell viability, proliferation, colony formation, migration, and invasion potential of lung cancer cells, whereas its knockdown showed the opposite effect. In addition, the levels of several proteins involved in the epithelial-to-mesenchymal transition negatively correlated with miR-590-5p levels in lung adenocarcinoma cells and tumors of NSCLC patients. Further, dual-luciferase reporter assays identified *STAT3* as a direct target of miR-590-5p, which negatively regulated STAT3 activation and its downstream signaling molecules (eg, Cyclin D1, c-Myc, Vimentin, and β-catenin) involved in tumorigenesis. Taken together, our study suggests that miR-590-5p functions as a tumor suppressor in NSCLC through regulating the STAT3 pathway, and may serve as a useful biomarker for the diagnosis/prognosis of NSCLC, and as a potential therapeutic target for the treatment of NSCLC.

KEYWORDS
circulating miRNA, liquid biopsy, miR-590-5p, non-small cell lung cancer, STAT3

1 | INTRODUCTION

In clinical practice, a biopsy is of paramount importance for the identification of lung tumor histology and its stage confirmation.[1] Currently, tissue biopsy, an invasive and time-consuming procedure, is often relied upon for confirmation of lung cancer, yet access to tissue samples is often limited due to the anatomical location of the tumors.[2-4] Further, to understand tumor progression

and the initial response to treatment, re-biopsy is often required; yet, the information obtained is often confounded by heterogeneity among the primary tumor and secondary metastases, thus limiting a clear representation of the disease profile.[5,6] Taking into account the limitations of using tissue biopsies, cell-free microRNAs (cf-miRNAs),[1] cell-free DNA (cfDNA),[7] cell-free long non-coding RNAs (cf-lncRNAs),[8,9] and circulating tumor cells (CTC)[10] that can be detected in liquid biopsies may provide a facile approach to obtain information on tissue-specific histology, stage, and metastatic status of the tumors.[2,3,11] Such an approach would provide a non-invasive, cost-effective procedure that has the potential to improve overall disease management. Therefore, liquid biopsy is greatly explored in current oncology research due to its minimally invasive approach for early cancer detection and for responses to cancer treatment.[3,12]

Circulating or cf-miRNAs disseminate from tumor tissue into the peripheral circulation[1] and are present in all body fluids, including whole blood, plasma, serum, sputum, saliva, urine, and cerebrospinal fluids.[2,13] These miRNAs are stable under harsh conditions, such as extreme pH, temperature, multiple freeze-thaw cycles, long-term storage, and even against RNase degradation.[14] In addition, they have the potential to serve as biomarkers for the diagnosis, staging, progression, and prognosis of cancer.[15] This is evident from several published reports that have shown the use of circulating miRNAs in early cancer detection, such as miR-196a in gastric cancer,[16] and the diagnostic roles of miR-106b-3p, miR-101-3p, and miR-1246 in hepatocellular carcinoma.[17] In lung cancer, low expression of the circulating miRNA-34 family was associated with clinicopathological status and poor progression-free and overall survival of NSCLC patients.[18] miR-223, miR-20a, miR-448, and miR-145, as serum/plasma miRNA signatures, have shown high sensitivity (>80%), whereas another panel including miR-628-3p, miR-29c, miR-210, and miR-1244 have shown high specificity (>90%) to stage I-II NSCLC samples.[19] Although several circulating miRNAs have been found to be associated with NSCLC, to date, their functional relevance in NSCLC has not been well characterized. Thus, a better understanding of the cellular functions of circulating miRNAs in NSCLC is warranted and may inform treatment responses.[2] Further, delineating their biological functions could prove pivotal in the clinical development of new liquid biopsy approaches in NSCLC.

With this goal in mind, the present study investigated circulating miR-590-5p dysregulation in blood plasma samples of NSCLC patients compared to non-cancerous healthy control plasma samples. miR-590-5p has been found to be dysregulated in various other cancers, such as colorectal,[20-22] hepatocellular,[23-25] breast,[26,27] cervix,[28] vulvar,[29] renal,[30,31] and gastric,[32,33] among others, and has been reported as both oncogenic and/or tumor suppressive. However, a role for circulating miR-590-5p dysregulation in lung cancer is not yet known; thus, we aimed to study its profile in NSCLC plasma samples and its clinical relevance. Additionally, we validated its target molecules, which take part in NSCLC progression and metastasis through activation of various cancer-associated pathways.

2 | MATERIALS AND METHODS

2.1 | Clinical sample and data collection

This study was conducted in accordance with the Declaration of Helsinki and was approved by the Ethics Committee at the Regional Cancer Centre, Indira Gandhi Medical College, Shimla, Himachal Pradesh, India and the Central University of Punjab, Bathinda, India. The blood samples from NSCLC patients and healthy individuals as controls were collected, and signed informed written consent was obtained from all the participants enrolled in the study. Each participant was assigned a unique code to maintain confidentiality of their information which was used only for the purposes of research.

Between July 2013 and July 2015, peripheral blood was collected from 80 patients diagnosed with NSCLC and 80 healthy individuals as controls following the inclusion and exclusion criteria. Only those patients who had not started treatment were enrolled in this study. Follow up of all the enrolled patients was done either by telephone or in person by the outpatient department of the hospital.

2.2 | Characteristics of participants

Non-small cell lung cancer patients were diagnosed based on histopathological examination of tissue biopsies according to the UICC and American Joint Committee on Cancer (AJCC) TNM staging 7th edition. Inclusion criteria for selection of NSCLC patients for the study included: (i) patients solely diagnosed with NSCLC before starting their treatment; (ii) histopathological stage confirmation as early or metastatic, adenocarcinoma or squamous cell carcinoma; (iii) patients' tumor grade between IA and IV; (iv) aged 18 years or above, and their gender information; (v) lifestyle history; number of pack-years (packs per day × years smoked) for current or former smokers (those who have quit smoking), non-smoker/passive smoker, and whether or not they consume alcohol and/or chew tobacco. Exclusion criteria for all NSCLC patients : (i) previous history or currently suffering from any disease; and (ii) currently taking medications.

Similarly, healthy individuals as controls with no history of cancer or other diseases were enrolled in the study. Inclusion criteria for selection of healthy individuals included: (i) individuals aged 18 years or above, and their gender information; (ii) lifestyle history; non-smoker, non-alcoholic, non-tobacco chewer. Exclusion criteria for such individuals: (i) previous cancer or any other disease history; (ii) currently taking medications. Clinical characteristics of the participants in this study are listed in Table 1.

2.3 | Circulating miRNA isolation, cDNA synthesis and qRT-PCR assay

Circulating miRNAs were isolated using the miRNeasy Serum/Plasma Kit (cat. no. 217184; Qiagen Inc.) as previously described.[34] Concentration of the isolated circulating miRNAs was assessed by using a NanoDrop 2000 UV-Vis Spectrophotometer (Thermo Fisher Scientific) and the samples were stored at −80°C until further use.

TABLE 1 Clinico-pathological features

Characteristics	No. of NSCLC patients (N = 80)	No. of healthy controls (N = 80)	*P*-value
TNM staging			
II	19	0	
III	54	0	
IV	7	0	
NSCLC types			
Adenocarcinoma	18	0	
Squamous cell carcinoma	41	0	
Mixed	21	0	
Lymph node metastasis			
Positive	56	0	
Negative	24	0	
Smoking status			
Yes	75	0	
No	5	0	
Alcoholic status			
Yes	52	0	
No	28	0	
Age			
≥50 y	67	48	<.0001
<50 y	13	32	.1148

The cDNA of isolated circulating miRNA samples was synthesized using the miScript II RT Kit (cat. no. 218161; Qiagen Inc.) as described previously.[35] These synthesized cDNAs were used as templates with which to carry out quantitative real-time PCR (qRT-PCR) reactions using the miScript SYBR Green PCR Kit (Qiagen Inc.) on a Bio-Rad CFX96 thermal cycler (Hercules). qRT-PCR reaction mixture (12.5 μL) was used for a miR-590-5p primer (cat. no. MS00004900; Qiagen Inc.) and a Spike-In control cel-miR-39 primer (cat. no. MS00019789; Qiagen Inc.) to determine technical variability in the samples. A non-template control reaction for each primer was also carried out to check for contamination by including all components except for the cDNA template. Conditions of qRT-PCR, including melt curves, were followed according to the manufacturer's instructions. Threshold cycle (Ct) value for each sample with both primers was recorded for statistical analysis. Gene expression of all the samples was calculated using the $2^{-\Delta Ct}$ method[36] where ΔCt = sample's average Ct value for miR-590-5p − sample's average Ct value for cel-miR-39. All reactions were repeated at least three independent times.

2.4 | Cell culture and transfection

Human NSCLC cell line, A549, was provided as a generous gift by Dr. Jayant (CDRI, India) and cultured in complete RPMI 1640 medium (Gibco, Thermo Fisher Scientific), supplemented with 10% FBS (Gibco, Thermo Fisher Scientific) and 1% PenStrep (Gibco, Thermo Fisher Scientific). All cells were maintained and incubated at 37°C in 5.0% CO_2 in a well-humidified incubator and were regularly checked for any type of contamination, whereas no *Mycoplasma* testing was done. For transfection, ~500 × 10^3 cells were cultured in six-well plates before 24 hours and miR-590-5p mimic (cat. no. MSY0003258) (200 mol L^{-1}) or miR-590-5p inhibitor (cat. no. MIN0003258) (5 mol L^{-1}) (Qiagen Inc.) was transfected with 4 μL Lipofectamine 3000 (Invitrogen, Thermo Fisher Scientific) in 500 μL Opti-MEM reduced serum media (Gibco, Thermo Fisher Scientific) to the respective well in the plates. For vehicle control, 4 μL Lipofectamine 3000 in 500 μL Opti-MEM reduced serum media was transfected in respective wells. Plates were incubated at 37°C in 5.0% CO_2 for 4 hours after transfection and then supplemented with 1.5 mL complete media, further incubated for 24 hours, 48 hours, and 72 hours for the subsequent experiments.

2.5 | Cell proliferation assay

Cells (6 × 10^3/well) were seeded in 96-well plates. After 24 hours of incubation, each well was transfected with either miR-590-5p mimic or inhibitor at different concentrations (between 0 and 200 mol L^{-1}) or vehicle control in Opti-MEM reduced serum media for 24-, 48- and 72-hour time points. MTT assay (Molecular Probes, Thermo Fisher Scientific) was carried out by measuring the absorbance at 570 nm using a BioTek Synergy H1 Hybrid Reader. The experiment was repeated at least three times. Data were expressed as the percentage of viable cells using the formula: relative cell viability (%) = (average absorbance (Abs.) of transfected cells/average Abs. of vehicle control transfected cells) × 100.

2.6 | Cell migration assay

After transfection with either the miR-590-5p mimic (200 mol L^{-1}), inhibitor (5 mol L^{-1}), or vehicle control in 70 μL Opti-MEM reduced serum media, 3.5 × 10^5 cells were seeded into each well of Culture-Insert 2 wells (Ibidi) placed in a respective μ-Dish (Ibidi). The insert was removed after cell attachment to obtain a 500-μm gap. Migration distance of the cells in the insert area was observed under an inverted microscope (Olympus) at 0 hours, 24 hours, and 48 hours until the gap was completely occupied by the migrating cells. Several different focuses were randomly selected at 4X magnification and photographed.

2.7 | Cell invasion assay

Cell invasion assays were carried out by using a CytoSelect Cell Invasion Assay kit (Cell Biolabs, Inc.) with polycarbonate membrane inserts (pore size, 8.0 μm) for A549 cells transfected with either miR-590-5p mimic (200 mol L^{-1}), inhibitor (5 mol L^{-1}), or vehicle control according to the manufacturer's protocol. After 48 h, invasive cells were observed under 10X magnification with an inverted microscope (Olympus). Relative numbers of invasive cells after extraction from the inserts were quantified at 560 nm using the BioTek Synergy

H1 Hybrid Reader. The experiments were repeated independently in triplicates.

2.8 | Cell cycle assay

A549 cells (500 × 10^3) were transfected with either the miR-590-5p mimic (200 mol L^{-1}), the inhibitor (5 mol L^{-1}), or vehicle control and harvested 48 hours post-transfection. The cell pellet was then fixed in 70% ice-cold ethanol and incubated at 4°C for 24 hours. After incubation, the cells were stained with FxCycle PI/RNase Staining Solution (Invitrogen, Thermo Fisher Scientific, USA) according to the manufacturer's protocol. Samples were analyzed with an Accuri C6 flow cytometer (BD Biosciences and analyzed using its supplied software.

2.9 | Cell apoptosis assay

A549 cells (500 × 10^3) were transfected either with miR-590-5p mimic (200 mol L^{-1}), the inhibitor (5 mol L^{-1}), or vehicle control and were incubated for 48 hours. After transfection and incubation, the cells were scraped and pelleted with their respective transfection media. The obtained pellet was washed three times in ice-cold 1X PBS. After washing, the cell pellet was resuspended in 500 μL of 1X Binding Buffer supplemented with the FITC Annexin V Apoptosis Detection Kit I (BD Pharmingen) and further processed according to the manufacturer's protocol. The samples were analyzed using an Accuri C6 (BD Biosciences) flow cytometer, equipped with software. Cells were discriminated into viable, early apoptotic, late apoptotic, and dead cells.

2.10 | Target gene prediction and pathway enrichment analysis

Online available computational algorithms, TargetScan version 7.2, DIANA-microT version 4, PITA, and miRDB, were used to identify the predicted targets of miR-590-5p. TarBase version 8 was used to confirm predicted targets with no previous experimental validation with respect to miR-590-5p.

2.11 | Immunoblot assay

Cell lysates were prepared from A549 cells and A549 cells transfected with miR-590-5p mimic (200 mol L^{-1}), miR-590-5p inhibitor (5 mol L^{-1}) or vector control. Approximately 20 μg protein extract was separated by 10% SDS-PAGE and transferred onto PVDF membranes (Bio-Rad Laboratories) using the Trans-Blot Turbo Transfer system (Bio-Rad Laboratories). Blots were incubated with primary antibodies in 1:1000 dilutions and incubated overnight at 4°C on an orbital shaker against anti-STAT3 (cat. no. S5933), anti-pSTAT3 (pSer727) (cat. no. SAB4300034), anti-Bcl-2 (cat. no. SAB4500003), anti-cMyc (cat. no. S4503662), anti-Cyclin D1 (cat. no. C7464) from Sigma-Aldrich; anti-Caspase 3 (cat. no. 9662), anti-Vimentin (cat. no. 5741), anti-β-catenin (cat. no. 8480), anti-Snail (cat. no. 3879), anti-TCF8/ZEB1 (cat. no. 3396), anti-E-cadherin (cat. no. 3195), anti-Claudin-1 (cat. no. 13255) and anti-Zo-1 (cat. no. 8193) from Cell Signaling Technologies. Anti-β-actin (cat. no. 4970; Cell Signaling Technologies) at a dilution of 1:3000 was used as a normalization and technical control. Blots were also incubated with HRP-conjugated secondary antibodies that were either anti-rabbit IgG (cat. no. 170-6515; Bio-Rad Laboratories) or anti-mouse IgG (cat. no. 170-6516; Bio-Rad Laboratories) at dilutions of 1:5000 and were imaged using Clarity Western ECL Substrate (Bio-Rad Laboratories) according to the manufacturer's instructions on a ChemiDoc Imaging System (Bio-Rad Laboratories) using ImageLab software (Bio-Rad Laboratories). Bands were quantified using ImageJ software (NIH).

2.12 | Immunohistochemistry

Formalin-fixed paraffin-embedded tumor tissue sections were immunostained with primary antibodies, including anti-STAT3 (1:50), anti-pSTAT3 (pSer727) (1:50), anti-Cyclin D1 (1:50) and anti-Vimentin (1:20), anti-β-catenin (1:50), anti-Snail (1:20; cat. no. 3879), anti-TCF8/ZEB1 (1:50), anti-E-cadherin (1:50). Immunohistochemistry experiments were carried out as previously described.[37] Immunostained positivity was defined and classified according to the respective protein expression in either the nucleus only, cytoplasm only, cell membrane only and/or combined; blindly confirmed by the pathologist. Microscopic images were processed using a Nikon microscope. Intensity score (IS) and proportion score (PS) was evaluated according to Cappuzzo et al.[38] For statistical analysis, total scores ranging between 0 and 200 were considered low expression, whereas those between 201 and 400 were considered high expression.

2.13 | Dual-luciferase reporter assay

For the dual-luciferase reporter assay, the 3′-UTR sequence of STAT3 (NM_003150) (cat. no. SC218770) containing the predicted binding sites for miR-590-5p and its corresponding mutated sequence (cat. no. CW304411) were cloned downstream of the *Renilla* luciferase gene in the vector pMirTarget named WT-3′-UTR STAT3 and MUT-3′UTR STAT3, respectively. These vectors along with pMirTarget expression vector (cat. no. PS100062) were purchased from Origene Technologies. Using Lipofectamine 3000 (Invitrogen, Thermo Fisher Scientific), HEK293T cells were cotransfected with reporter plasmids and miR-590-5p mimics (200 mol L^{-1}), or a negative control. Luciferase activity was determined after 48 hours incubation using the Dual-Luciferase Reporter Assay System (cat. no. E1910; Promega) and GloMax 20/20 luminometer (cat. no. E5311; Promega). HEK-293T cells were subjected to dual-luciferase activity by normalizing with *Renilla* luciferase activity according to the manufacturer's instructions. Normalized data were measured as the ratio of experimental (*Renilla*) luciferase to control (Firefly) luciferase. Each experiment was repeated at least three times.

2.14 | Statistical analysis

All statistical analyses were carried out using GraphPad Prism software 7.0. Data are presented as either mean ± standard deviation (SD) or mean ± standard error mean (SEM). Overall survival was evaluated by the Kaplan-Meier method with a log-rank test for comparison between miR-590-5p high-expression and low-expression groups. "High" and "low" expression was based on the median value of miR-590-5p expression, which was used as the cut-off value. $P \leq .05$ was considered statistically significant.

3 | RESULTS

3.1 | Circulating miR-590-5p expression negatively correlates with NSCLC pathogenesis

A total of 80 NSCLC patients were enrolled in this study. The NSCLC cohort (n = 80) consisted of individuals with a median age of 55 ± 14.95 years in the range 40-70 years, and an age-matched healthy control cohort (n = 80) with a median age of 50.50 ± 15.50 years in the range 34-66 years. Within the NSCLC cohort, study subjects were segregated on the basis of their staging; for example, stage II (n = 19) 23.75% with a median age of 56 ± 13.10 years, stage III (n = 54) 67.5% with a median age of 52 ± 12.90 years, and stage IV (n = 7) 8.75% with a median age of 64 ± 5.70 years.

Previous studies have found dysregulation of miR-590-5p in a number of different types of cancer cells.[20-22,24,26-29,31,33] Thus, we examined the correlation of miRNA with disease progression of NSCLC. We compared the levels of circulating miR-590-5p in plasma samples from NSCLC patients and healthy controls and found that the average expression level of circulating miR-590-5p was significantly downregulated (~7.5-fold) ($P < .0001$; 95% CI: 0.4151-1.077) in blood plasma samples of NSCLC patients compared to healthy controls (Figure 1), suggesting a negative correlation of miR-590-5p with NSCLC disease progression.

3.2 | Low expression of circulating miR-590-5p is associated with clinicopathological features and poor prognosis of NSCLC patients

Considering the significant downregulation of circulating miR-590-5p expression levels in plasma samples of NSCLC patients compared to healthy controls, we evaluated the correlation between miR-590-5p expression and clinicopathological features such as age, smoking history, lymph node metastasis, and TNM staging. Among different NSCLC stages, patients with TNM stage II (n = 19) showed significant downregulation of miR-590-5p (~10-fold) ($P = .0306$; 95% CI: 0.07404-1.476) compared to healthy controls, whereas stage III (n = 54) NSCLC patients showed the most significant downregulation by approximately seven-fold ($P = .0005$; 95% CI: 0.3332-1.148) (Figure 2A). Patients with stage IV (n = 7) also showed a marginal downregulation compared to healthy controls, (Figure 2A). When we compared the expression levels of miR-590-5p among various TNM staging of NSCLC patients, no

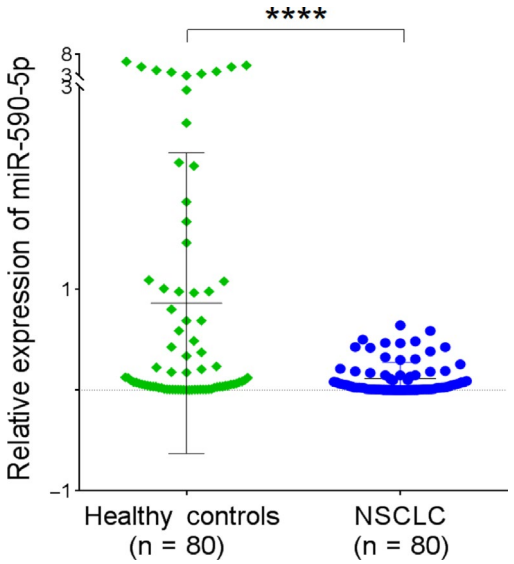

FIGURE 1 Circulating microRNA (miR)-590-5p expression levels in plasma samples were downregulated in non-small cell lung cancer (NSCLC) patients compared to healthy controls. Scatter plot represents normalized $2^{-\Delta Ct}$ values of individual samples from n = 3 independent qRT-PCR experiments. Data are expressed as mean ± SD. ****$P < .0001$ calculated using an unpaired *t* test

significant changes were observed between stages, suggesting that circulating miR-590-5p was expressed at similar levels in all NSCLC stages. Next, we analyzed the expression levels of miR-590-5p on the basis of NSCLC type, and we found that significant downregulation (~9-fold) occurred in squamous cell carcinoma (n = 41; $P = .0014$; 95% CI: 0.3045-1.231), an approximate six-fold downregulation in adenocarcinoma (n = 18; $P = .0459$; 95% CI: 0.01318-1.416), and an approximate sevenfold downregulation in the mixed-type NSCLC (n = 21, $P = .0276$; 95% CI: 0.08239-1.381) (Figure 2B). As all groups were similarly downregulated, we did not observe any significant differences in expression between the various NSCLC types studied. NSCLC patients with both lymph node-positive (n = 56) and -negative (n = 24) NSCLC showed significant downregulation of miR-590-5p, where lymph node-positive patients showed an approximate seven-fold change ($P = .0003$; 95% CI: 0.3447-1.130) and lymph node-negative patients showed an approximate nine-fold change ($P = .0137$; 95% CI: 0.1604-1.374) compared to healthy controls (Figure 2C).

miR-590-5p expression levels were also reduced significantly in NSCLC patient with smoking habits (n = 75; $P < .0001$; 95% CI: 0.4093-1.093), whereas no significant changes were observed statistically in non-smokers compared to healthy controls (Figure 2D). Similarly, miR-590-5p expression levels were significantly reduced in alcoholic patients (n = 52; $P = .0003$; 95% CI: 0.3675-1.189) along with non-alcoholic patients (n = 28; $P = .0170$; 95% CI: 0.1251-1.249) (Figure 2E). Patients over 50 years showed significant downregulation of miR-590-5p by approximately nine-fold (n = 67; $P < .0001$; 95% CI: 0.4009-1.124), whereas no statistically significant change ($P = .1148$) was seen in patients below 50 years compared to healthy controls (Figure 2F). Taken together, the above data suggested that the expression levels of miR-590-5p negatively correlated with

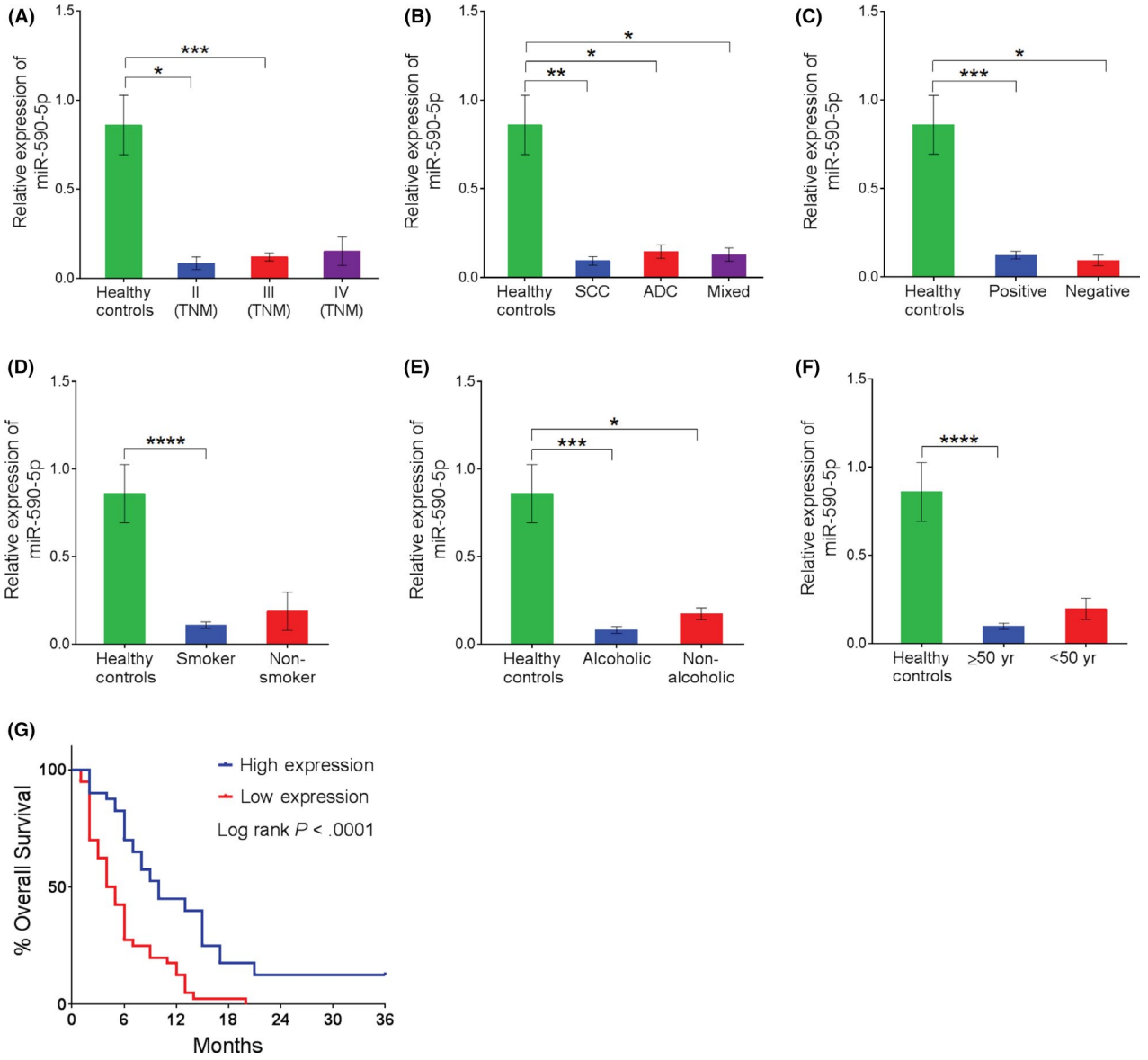

FIGURE 2 Circulating microRNA (miR-590-5p) expression correlated with clinicopathological features of non-small cell lung cancer (NSCLC) patients. A, TNM stages of NSCLC patients. B, NSCLC histological types. C, Lymph node status of NSCLC patients. D, Smoking status of NSCLC patients. E, Alcoholic status of NSCLC patients. F, Age of NSCLC patients. G, Kaplan-Meier survival test to determine relationships between levels of miR-590-5p expression and percentage of overall survival of NSCLC patients. Bar graph represents normalized $2^{-\Delta Ct}$ values from three independent experiments. Data are expressed as mean ± SEM. *P < .05, **P < .01, ***P < .001, ****P < .0001 calculated using unpaired t tests. ADC, adenocarcinoma; SCC, squamous cell carcinoma

FIGURE 3 MicroRNA (miR)-590-5p inhibits non-small cell lung cancer (NSCLC) cell proliferation and affects cell cycle progression and apoptosis, as assessed by transfecting miR-590-5p inhibitor and mimics in A549 cells. A, Cell proliferation was assessed by MTT assays at 24-, 48-, and 72-h time points in A549 cells transfected with vehicle control, an miR-590-5p inhibitor (5 mol L^{-1}), or a miR-590-5p mimic (200 mol L^{-1}). B, Colony formation assay for A549 cells transfected with vehicle control, inhibitor (5 mol L^{-1}), or mimic (200 mol L^{-1}). C, Cell cycle analysis was carried out by flow cytometry of A549 cells transfected with vehicle control, inhibitor (5 mol L^{-1}), or mimic (200 mol L^{-1}). D, Apoptosis was assessed by flow cytometry of A549 cells transfected with vehicle control, inhibitor (5 mol L^{-1}), or mimic (200 mol L^{-1}). E, A549 cells were transfected with vehicle control, inhibitor (5 mol L^{-1}), or mimic (200 mol L^{-1}) to determine normalized protein levels of Cyclin D1, Bcl-2 and Caspase 3 as assessed by immunoblotting. All experiments were carried out three independent times. Values and bar graphs are presented as mean ± SEM where *P > .05, **P < .05 represent significant differences from vehicle control calculated using paired t tests. F, Immunohistochemistry shows brown-stained positive tumor cells in the nucleus, the cytoplasm, and/or the cell membrane, representing protein levels of Cyclin D1 in NSCLC patient tissues. Scale bar, 100 μm and n = 3 NSCLC tissues

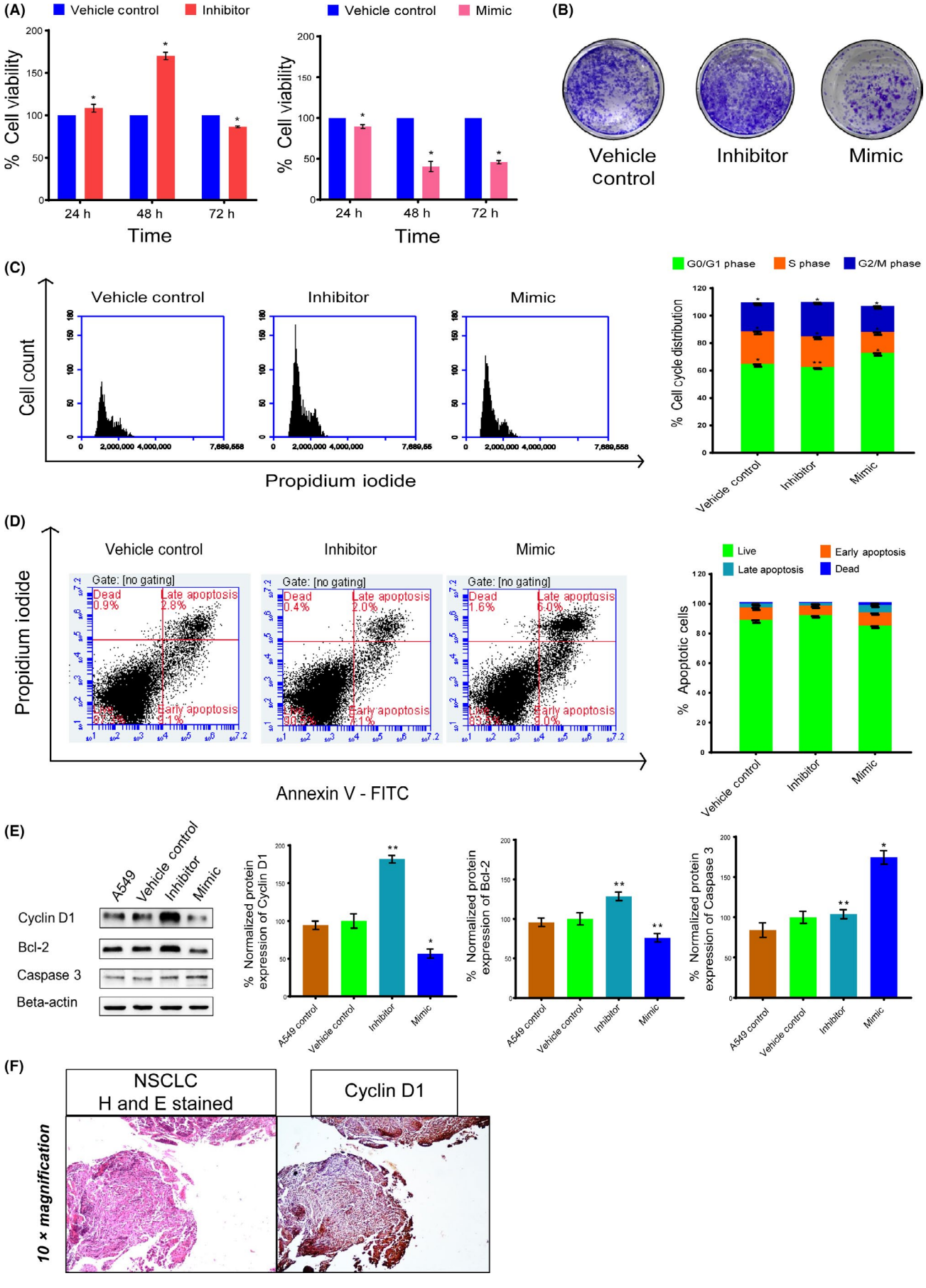
(A)
Vehicle control
Inhibitor
Vehicle control
Mimic
% Cell viability
Time
24 h
48 h
72 h
(B)
Vehicle control
Inhibitor
Mimic
(C)
Vehicle control
Inhibitor
Mimic
Cell count
Propidium iodide
G0/G1 phase
S phase
G2/M phase
% Cell cycle distribution
(D)
Propidium iodide
Annexin V - FITC
Gate: [no gating]
Dead 0.9%
Late apoptosis 2.8%
Early apoptosis 9.1%
Dead 0.4%
Late apoptosis 2.0%
Early apoptosis 7.1%
Dead 1.6%
Late apoptosis 6.0%
Early apoptosis 9.0%
Live
Early apoptosis
Late apoptosis
Dead
% Apoptotic cells
(E)
A549
Vehicle control
Inhibitor
Mimic
Cyclin D1
Bcl-2
Caspase 3
Beta-actin
% Normalized protein expression of Cyclin D1
% Normalized protein expression of Bcl-2
% Normalized protein expression of Caspase 3
A549 control
(F)
NSCLC
H and E stained
Cyclin D1
10 × magnification

various clinicopathological features of NSCLC patients, including smoking and alcohol history.

To further investigate the association of miRNA-590-5p expression with prognosis of NSCLC patients, Kaplan-Meier and log-rank analyses were used to evaluate the effects of miR-590-5p expression on overall patient survival. We found that patients with low miR-590-5p expression had significantly lower median survival rates in comparison to patients expressing high miR-590-5p levels ($P < .0001$; 95% CI: 1.412-3.498) (Figure 2G). Together, these findings identified a negative correlation of miR-590-5p in the prognosis of NSCLC patients, and suggested that miR-590-5p may function as a tumor suppressor in NSCLC development.

3.3 | MicroRNA-590-5p inhibits NSCLC cell proliferation and affects cell cycle progression and apoptosis

A characteristic hallmark of many cancer cells is their uncontrolled cell proliferation and resistance to apoptotic signals. On the basis of the results mentioned above, we further assessed how miR-590-5p might regulate cell proliferation and apoptosis in lung tumor cells. To this purpose, we transfected human A549 adenocarcinoma lung cancer cells with either a miR-590-5p inhibitor (5 mol L^{-1}) or a miR-590-5p mimic (200 mol L^{-1}) as mentioned in the Materials and Methods. By using MTT assays, we observed that A549 cells transfected with the inhibitor showed an ~70% increase in viability, whereas those treated with the mimic showed an ~60% decrease in viability 48 hours post-transfection (Figure 3A). Further, through colony formation assays, we detected an increase in both size and number of colonies in the A549 cells transfected with the inhibitor, and the opposite for the mimic-transfected A549 cells compared to the vehicle control (Figure 3B). Taken together, the results from both assays indicated that miR-590-5p decreased growth and proliferation of A549 cells. As the maximum changes were observed at 48 hours post-transfection, this time point was used for subsequent assays.

We next evaluated the influence of miR-590-5p on cell cycle regulation. Cell cycle analyses showed significant cell cycle arrest in A549 cells harboring high levels of miR-590-5p. In contrast, depletion of miR-590-5p caused an accumulation of these cells in the S and G2/M phases, and significantly reduced the number of cells in the G0/G1 phase by ~61% (Figure 3C). Further, increased levels of miR-590-5p in the A549 cells treated with the mimic resulted in increased cell death compared to cells containing lower levels of this miRNA (Figure 3D), which was further evident by changes in the levels of both anti- and pro-apoptotic factors (Figure 3E), and Cyclin D1 (Figure 3F). Consistent with these findings, immunohistochemistry (IHC) analysis of NSCLC patient tissue samples also showed Cyclin D1 positivity (Figure 3E,F) in as much as 60% of the tumor cells. Taken together, these results suggested that miR-590-5p played a role in NSCLC suppression by inhibiting cell growth and inducing apoptosis.

3.4 | MicroRNA-590-5p influences multistage carcinogenic programming in tumor cells

Cell migration and invasion are crucial for cancer progression and, based on the results above, we expected a correlation of miR-590-5p with these processes. Thus, we assessed the influence of miR-590-5p on cell migration and invasive potential of A549 cells. Results showed increased migration of cells transfected with the inhibitor, whereas lower levels of cell migration were observed when transfected with the mimic, compared to the A549 control and vehicle control cells (Figure 4A). Similarly, when miR-590-5p was depleted, more cells (~3-fold) were able to invade the matrix and polycarbonate membranes after 48 hours compared to the control cells (Figure 4B).

Results from the experiments described above suggested that miR-590-5p influenced the processes of migration and invasion of NSCLC cells. In order to substantiate this, we analyzed the impact of temporal changes of miR-590-5p levels with the epithelial-to-mesenchymal transition (EMT), which plays a critical role in cancer progression. Indeed, depletion of miR-590-5p resulted in increased protein levels of the mesenchymal markers, Vimentin, Snail, TCF8/ZEB1, and β-catenin by ~65%, 40%, 85% and 66%, respectively, whereas its overexpression significantly increased the levels of epithelial markers, such as E-cadherin, Zo-1, and Claudin-1 by ~100%, ~60%, and ~50%, respectively, compared to the vehicle control-treated cells. As expected, increased levels of miR-590-5p had an opposite effect on the levels of these proteins (Figure 4C). Thus, these results suggested that miR-590-5p modulated the invasion and migration of tumor cells through EMT pathways. IHC analysis of EMT proteins in NSCLC patient tumor samples showed that a significant proportion of the tumor cells were positive for various proteins, such as β-catenin (78%); Snail (96%), TCF8/ZEB1 (72%), and E-cadherin (85%) (Figure 4D), thus supporting the involvement of these proteins in NSCLC progression.

FIGURE 4 MicroRNA (miR)-590-5p influences cell migration, invasion, and epithelial-mesenchymal transition (EMT). A, Cell migration assays were carried out with A549 cells transfected with vehicle control, an inhibitor, or a mimic at 0-, 24-, and 48-h time points. B, Cell invasion capacity of A549 cells was assessed in cells transfected with vehicle control, inhibitor, or a mimic at 48 h after transfection. All experiments were carried out three independent times. Values and bar graphs are presented as mean ± SEM where $^{*}P > .01$, $^{**}P < .001$ represent significant differences from vehicle control calculated using paired *t* tests. C, A549 cells were transfected with vehicle control, an inhibitor (5 mol L^{-1}), or a mimic (200 mol L^{-1}) to measure normalized protein levels of EMT-regulated proteins: Vimentin, β-catenin, TCF8/ZEB1, Snail, E-cadherin, Claudin-1, Zo-1 as assessed by immunoblotting. All experiments were carried out four independent times where values and bar graphs represent mean ± SEM. $^{*}P > .05$, $^{**}P < .05$ represent significant differences from vehicle control calculated using paired *t* tests. D, Immunohistochemistry shows brown-stained positive tumor cells in the nucleus (N), cytoplasm (C), and/or cell membrane (M), representing protein levels of β-catenin, Vimentin, E-cadherin, Snail, and TCF8/ZEB1 in non-small cell lung cancer (NSCLC) patient tissues. Scale bar, 100 μm and n = 3 NSCLC tissues

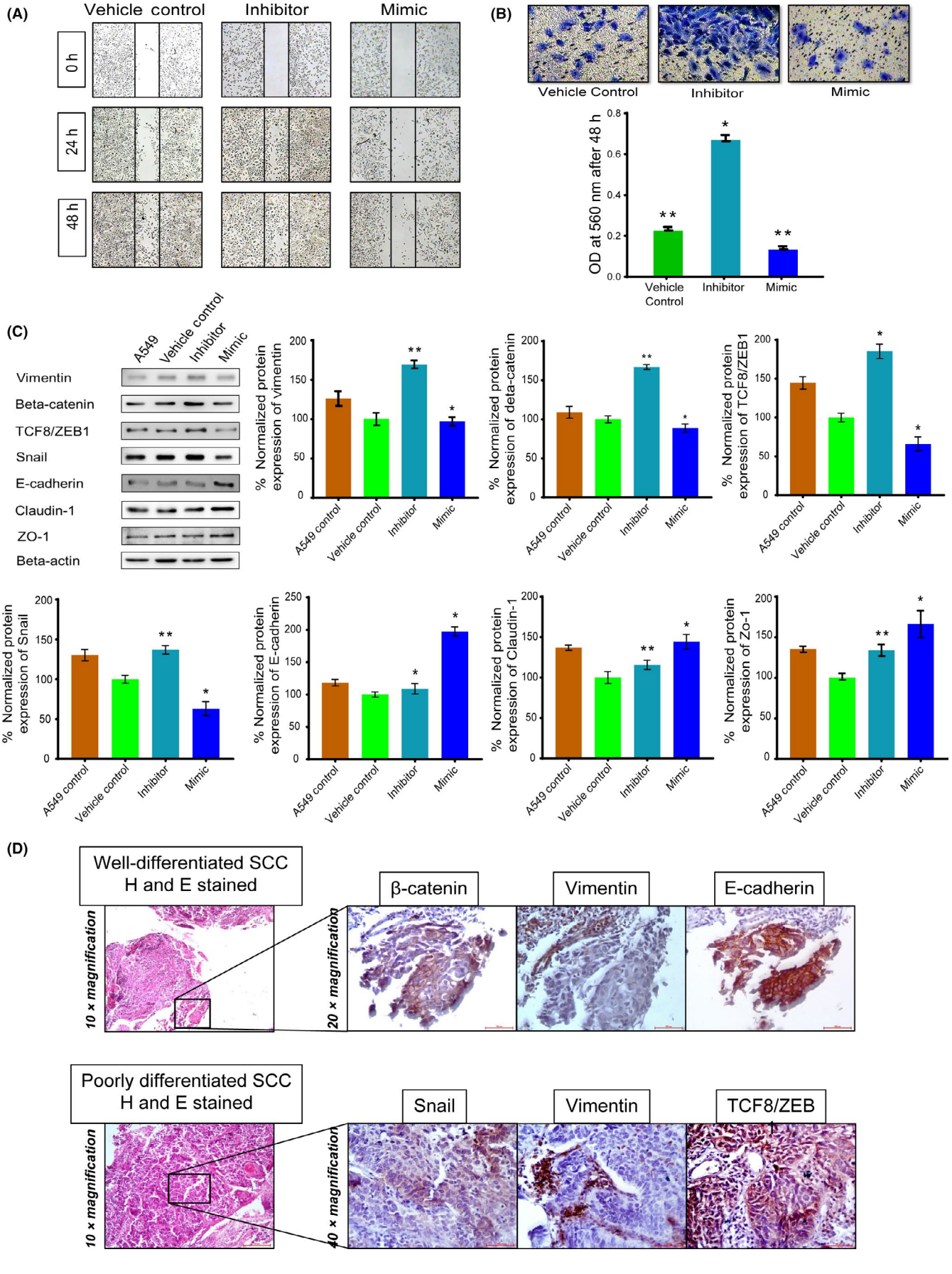
(A)
Vehicle control
Inhibitor
Mimic
0 h
24 h
48 h
(B)
Vehicle Control
Inhibitor
Mimic
OD at 560 nm after 48 h
Vehicle Control
Inhibitor
Mimic
(C)
A549
Vehicle control
Inhibitor
Mimic
Vimentin
Beta-catenin
TCF8/ZEB1
Snail
E-cadherin
Claudin-1
ZO-1
Beta-actin
% Normalized protein expression of Vimentin
% Normalized protein expression of deta-catenin
% Normalized protein expression of TCF8/ZEB1
% Normalized protein expression of Snail
% Normalized protein expression of E-cadherin
% Normalized protein expression of Claudin-1
% Normalized protein expression of Zo-1
A549 control
Vehicle control
Inhibitor
Mimic
(D)
Well-differentiated SCC
H and E stained
10 × magnification
20 × magnification
β-catenin
Vimentin
E-cadherin
Poorly differentiated SCC
H and E stained
10 × magnification
40 × magnification
Snail
Vimentin
TCF8/ZEB

3.5 | *STAT3* is a direct target of miR-590-5p

MicroRNAs function by binding and regulating their target protein-coding RNAs, which can function as oncogenes or tumor suppressors. Therefore, to gain insight into the molecular mechanisms of miR-590-5p in the progression of NSCLC, publicly available algorithms were used to predict its possible targets. TargetScan, DIANA-microT, PITA and miRDB predicted 70 common possible targets, analyzed by Venny 2.1 (http://bioinfogp.cnb.csic.es/tools/venny/) (Figure 5A). From the list of predicted target mRNA molecules, *STAT3* was identified as one of its potential targets, binding at its 3′UTR (Figure 5B). It is well known that STAT3 plays a significant role in the progression of lung cancer, and has also been found to be a key protein in NSCLC through the Kyoto Encyclopedia of Genes and Genomes (KEGG) database. Therefore, to verify whether miR-590-5p directly regulated *STAT3*, we carried out a dual-luciferase reporter assay and found that the miR-590-5p mimic (200 mol L^{-1}) significantly inhibited (~55%, $P < .05$) luciferase activity in HEK293T cells transfected with the pMirTarget WT-3′UTR STAT3 reporter plasmid compared to control cells transfected with an empty vector (Figure 5C). As expected, the activity remained unaffected in the HEK293T cells transfected with the pMirTarget MUT-3′UTR STAT3 mutated plasmid (Figure 5C). Thus, these results indicated that *STAT3* is a direct target of miR-590-5p.

To determine the effect of miR-590-5p on STAT3, both total STAT3 and phosphorylated STAT3 (pSTAT3 at Ser727) protein levels were assessed by immunoblotting. Notably, in the miR-590-5p inhibitor-transfected A549 cells, expression levels of both STAT3 and pSTAT3 increased by ~45% and ~55%, respectively, whereas both were decreased by ~40% when A549 cells were transfected with its mimic compared to A549 control and vehicle control cells after 48 hours (Figure 6A). These results suggested a negative correlation of miR-590-5p with STAT3 protein in NSCLC cells, consistent with our results showing that ~90% of tumor cells were positive for STAT3 in the cytoplasm, and ~82% of the tumor cells were positive for pSTAT3 in both the nucleus and cytoplasm (Figure 6B).

Because we found an effect of miR-590-5p in regulating *STAT3*, we also examined its effects on two STAT3 downstream targets, *Cyclin*

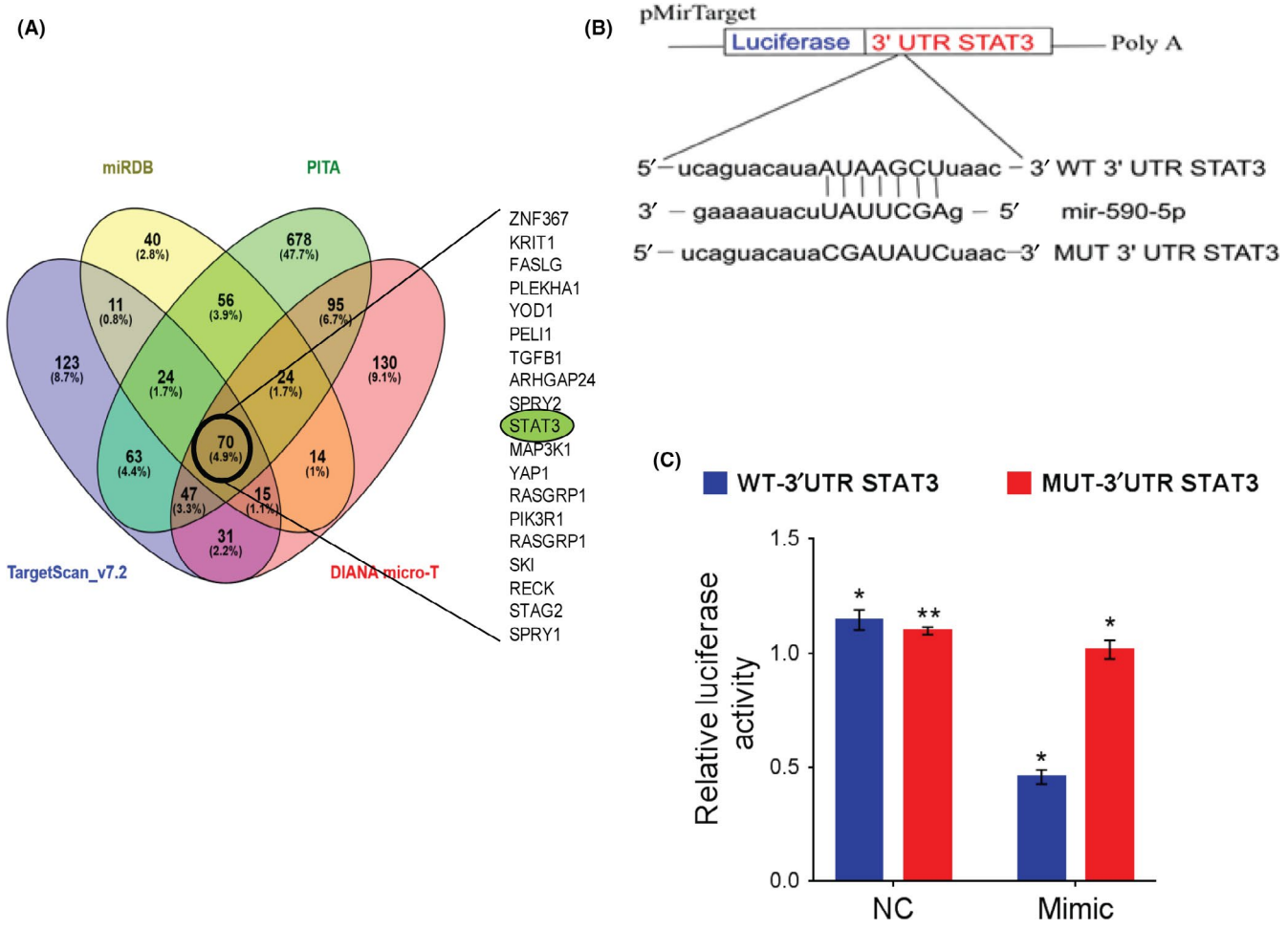

FIGURE 5 *STAT3* is a target of microRNA (miR)-590-5p in non-small cell lung cancer (NSCLC) cells. A, In silico target prediction of miR-590-5p. Seventy common targets of miR-590-5p (highlighted by a black circle) resulted from different databases: TargetScan version 7.2 (blue), DIANA micro-T (pink), PITA (green), and miRDB (peach). B, Predicted miR-590-5p binding sites with the 3′UTR of *STAT3* as assessed by the online bioinformatics tool DIANA micro-T. C, Detection of miR-590-5p regulation of *STAT3* using a dual-luciferase reporter assay. Data are shown as mean ± SEM of triplicate experiments, where $*P > .05$, $**P < .05$ represent significant difference calculated using paired *t* tests. NC, negative control

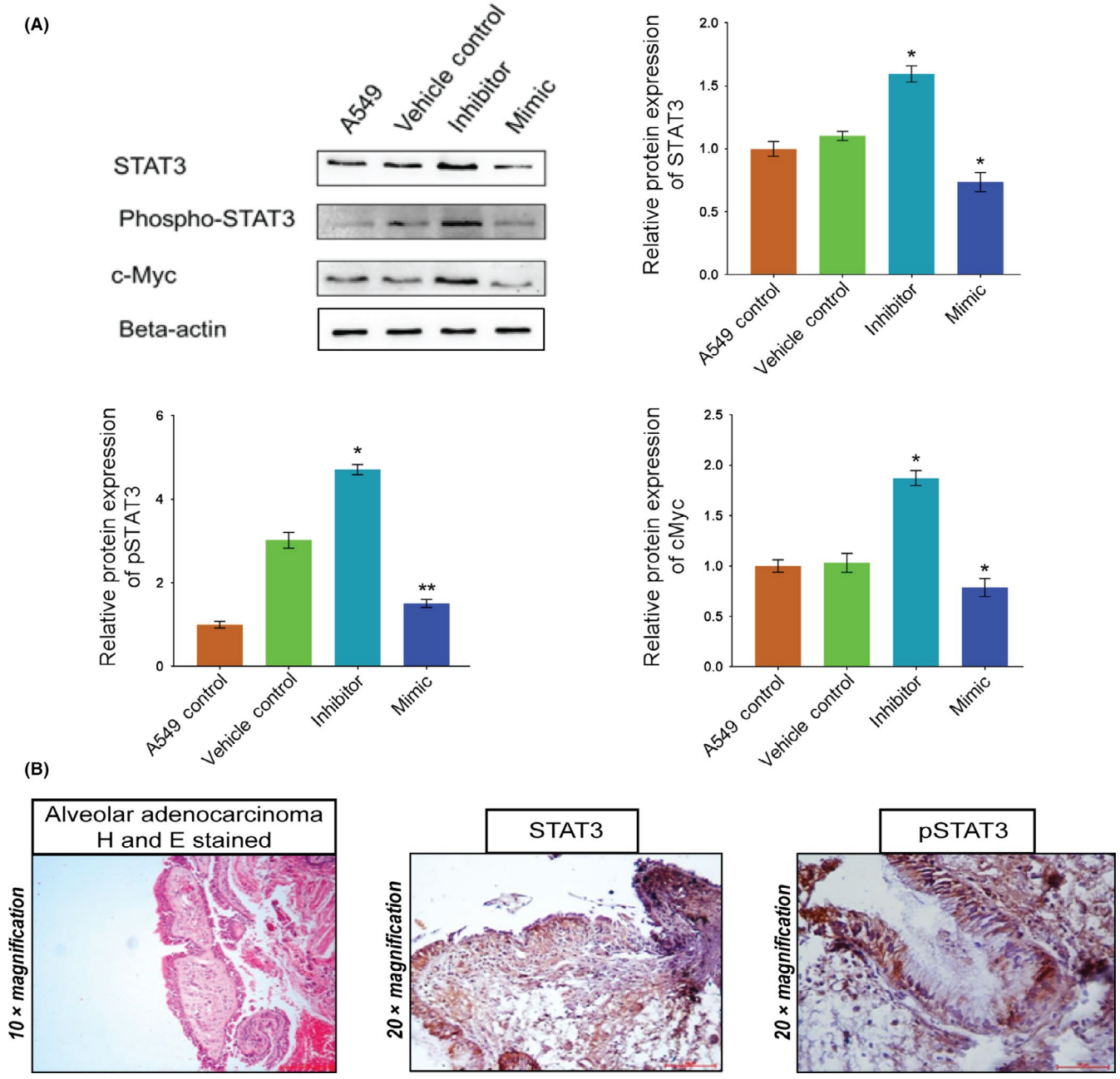

FIGURE 6 Regulation of STAT3 and its downstream targets by microRNA (miR)-590-5p. A, Immunoblot assays were used to determine normalized protein levels of STAT3, Phospho-STAT3 (pSTAT3^{pSer727}) and c-Myc in A549 cells, and A549 cells transfected with vehicle control, a miR-590-5p inhibitor (5 mol L^{-1}), or a miR-590-5p mimic (200 mol L^{-1}). All experiments were carried out four independent times where values and bar graphs represent mean ± SEM. *P > .05, **P < .05 represent significant differences from vehicle control calculated using paired t tests. B, Immunohistochemistry shows brown-stained positive tumor cells in the nucleus, the cytoplasm, and/or both, representing protein levels of STAT3 and pSTAT3 in NSCLC patient tissues. Scale bar, 100 μm and n = 3 NSCLC tissues

D1 and *c-Myc*, which also play roles in cell proliferation and cell cycle progression. We studied the effects of miR-590-5p suppression and overexpression on the protein levels of these two downstream targets of STAT3, and found that they were upregulated when A549 cells were transfected with its inhibitor, and downregulated when transfected with its mimic, similar to the STAT3 and pSTAT3 protein levels (Figures 3E and 6A). Moreover, IHC analysis also showed high expression of Cyclin D1 in NSCLC patient tissue samples (Figure 3F).

4 | DISCUSSION

Recently, cellular miR-590-5p has been shown to play important roles in tumorigenesis and metastasis of various cancers where it was shown to function as either a tumor suppressor or an oncomiR based on its target(s) in the respective cancers. Its expression was found to be downregulated in breast, hepatocellular, colorectal, and lung cancer tissues, and targeted the Wnt/β-catenin pathway, SOX2 (SRY-box

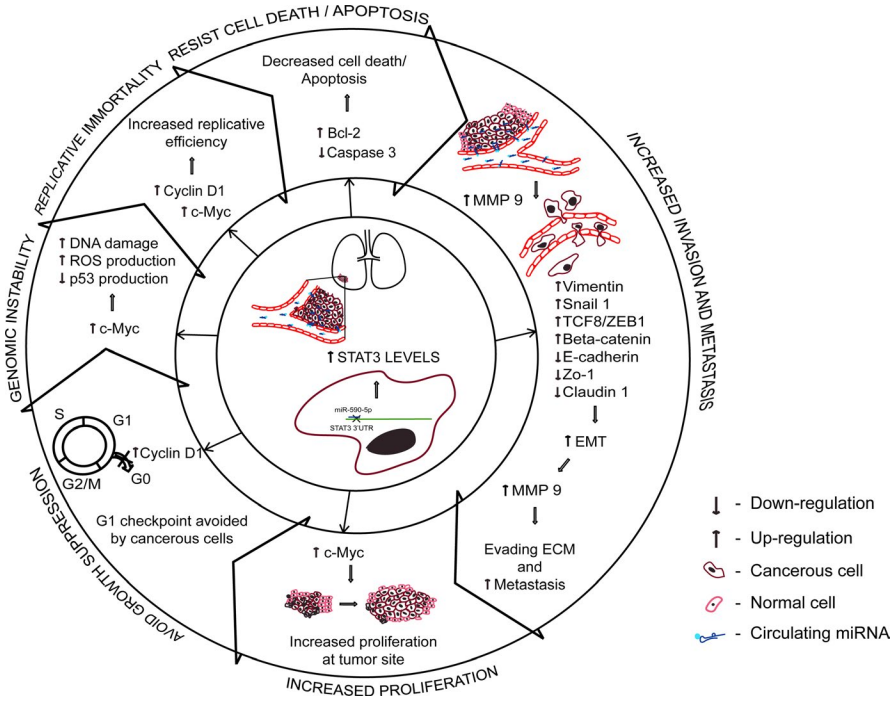

FIGURE 7 Schematic diagram of various cancer hallmarks and molecules regulated by microRNA (miR)-590-5p in non-small cell lung cancer. Various upregulated and downregulated molecules and pathways are depicted by up and down arrows, respectively. ECM, extracellular matrix; EMT, epithelial-to-mesenchymal transition

2), TGF-βRII (transforming growth factor beta receptor 2),[23] NF90/VEGFA (nuclear factor 90/vascular endothelial growth factor A)[20,21] and GAB1 (GRB2 associated binding protein A)[39] which promote cancer growth and progression.[22,26,27,40,41] Likewise, miR-590-5p oncogenic properties were reported in gastric, cervical, vulvar, and clear cell renal cancer, where it targets RECK (reversion inducing cysteine rich protein with kazal motifs),[32] CHL1 (close homolog of L1),[28] TGF-βRII,[29] and PBRM1 (Polybromo 1),[30] respectively, and regulates cell proliferation, migration and invasion of cancer cells. However, the role of circulating miR-590-5p in blood plasma has not been reported. Herein, we observed that circulating miR-590-5p was downregulated (~7.5-fold) in NSCLC patient plasma samples which correlated with their clinicopathological features, whereas its upregulation reflected prolonged survival over its low expression levels.

Mechanistically, we showed *STAT3* as a direct downstream target gene of miR-590-5p. STAT3 is a transcription factor known to regulate various cellular signaling pathways involved in cancer progression.[42] In NSCLC, upregulated transcripts and protein levels of STAT3 were reported to be associated with lymph node metastasis,[43] poor prognosis,[28,44] tumor differentiation,[44] and downregulation of miR-124.[45] miR-590-5p showed an inverse correlation with constitutive STAT3 and phosphorylated STAT3 in the present study, and highlighted the significance of miR-590-5p in STAT3-dependent tumor progression. As STAT3 pathways constituting signaling networks are important for tumor progression, our results suggest that the miR-590-5p-STAT3 axis may function as a signaling pathway by which miR-590-5p could influence tumor growth. Various proteins such as interleukin (IL)-6, JAK1/2, epidermal growth factor receptor (EGFR), and Src directly activate STAT3 and phosphorylate it at Tyr705. Studies have also shown that phosphorylation of STAT3 at Ser727, present in its transactivating C-terminal domain,[46] enhances the constitutive phosphorylation of STAT3 at Tyr705 in both the nucleus and the cytoplasm. pSTAT3 at Ser727 has also been reported to increase its DNA-binding ability, and thereby control transcriptional activity of cancerous cells[47,48] and activate other downstream targets, such as *Cyclin D1*,[44] *Bcl-2*, *c-Myc*, *Vimentin*, *TCF8/ZEB1*, etc. that regulate oncogenic pathways.[49] In line with this, we observed a negative correlation of miR-590-5p levels with increased Cyclin D1, Bcl-2 and decreased Caspase 3 protein levels (Figure 3E) in miR-590-5p inhibitor-transfected A549 cells. Similarly, c-Myc protein levels were upregulated upon inhibiting endogenous miR-590-5p levels (Figure 6A), along with increased cellular proliferation (Figure 3A,B).

Another important factor in cancer progression is an EMT phenotype,[50] which is critical for tumor metastasis. Increasing evidence has suggested that STAT3 is responsible for the occurrence and metastasis of cancer involving the regulation of EMT[51] through its activation by IL-17 and TGF-β.[52,53] Along these lines, an inverse correlation of circulating miR-590-5p levels with EMT regulatory protein such as Vimentin, TCF8/ZEB1, β-catenin, and Snail1 of mesenchymal origin was found. Moreover, we detected decreased levels of E-cadherin, Claudin-1 and Zo-1 in NSCLC patient tissue samples reflecting the migration and invasion potential of NSCLC cells. Thus, downregulation of circulating miR-590-5p increased EMT, perhaps by upregulation of *STAT3*, thereby promoting NSCLC progression.

In summary, we showed that circulating miR-590-5p functions as a tumor suppressor in NSCLC by regulating various hallmarks of cancer, such as cell proliferation, migration, invasion, apoptosis, and EMT (Figure 7). Thus, determining the circulating levels of miR-590-5p could potentially be used as a diagnostic marker for NSCLC, which might prove to be a potential target in NSCLC management. Further investigations with additional patient samples may

provide further support for circulating miR-590-5p as a biomarker for improved diagnosis, prognosis, and as a potential therapeutic target for NSCLC patients.

ACKNOWLEDGMENTS

A.J. would like to acknowledge support from the Indian Council of Medical Research (5/13/81/2013-NCD-III). This work was also supported by NIH/NCI grant (CA093729) to K.M.V.

CONFLICTS OF INTEREST

Authors declare no conflicts of interest for this article.

ORCID

Aklank Jain https://orcid.org/0000-0001-5539-3225

REFERENCES

1. Hou J, Meng F, Chan LW, Cho WC, Wong SC. Circulating plasma MicroRNAs as diagnostic markers for NSCLC. *Front Genet*. 2016;7:193.
2. Inamura K. Diagnostic and therapeutic potential of MicroRNAs in lung cancer. *Cancers*. 2017;9.
3. Matikas A, Syrigos KN, Agelaki S. Circulating biomarkers in non-small-cell lung cancer: current status and future challenges. *Clin Lung Cancer*. 2016;17:507-516.
4. Taverna S, Giallombardo M, Gil-Bazo I, et al. Exosomes isolation and characterization in serum is feasible in non-small cell lung cancer patients: critical analysis of evidence and potential role in clinical practice. *Oncotarget*. 2016;7:28748-28760.
5. Xu-Welliver M, Carbone DP. Blood-based biomarkers in lung cancer: prognosis and treatment decisions. *Transl Lung Cancer Res*. 2017;6:708-712.
6. Mamdani H, Ahmed S, Armstrong S, Mok T, Jalal SI. Blood-based tumor biomarkers in lung cancer for detection and treatment. *Transl Lung Cancer Res*. 2017;6:648-660.
7. Martinez-Ricarte F, Mayor R, Martinez-Saez E, et al. Molecular diagnosis of diffuse gliomas through sequencing of cell-free circulating tumor DNA from cerebrospinal fluid. *Clin Cancer Res*. 2018;24:2812-2819.
8. Du L, Duan W, Jiang X, et al. Cell-free lncRNA expression signatures in urine serve as novel non-invasive biomarkers for diagnosis and recurrence prediction of bladder cancer. *J Cell Mol Med*. 2018;22:2838-2845.
9. Khandelwal A, Bacolla A, Vasquez KM, Jain A. Long non-coding RNA: a new paradigm for lung cancer. *Mol Carcinog*. 2015;54:1235-1251.
10. Hua G, Yanjiao H, Qian L, Jichao W, Yazhuo Z. Detection of circulating tumor cells in patients with pituitary tumors. *BMC Cancer*. 2018;18:336.
11. Mambetsariev I, Vora L, Yu KW, Salgia R. Effective osimertinib treatment in a patient with discordant T790 M mutation detection between liquid biopsy and tissue biopsy. *BMC Cancer*. 2018;18:314.
12. Castellanos-Rizaldos E, Grimm DG, Tadigotla V, et al. Exosome-based detection of EGFR T790M in plasma from non-small cell lung cancer patients. *Clin Cancer Res*. 2018;24:2944-2950.
13. Mitchell PS, Parkin RK, Kroh EM, et al. Circulating microRNAs as stable blood-based markers for cancer detection. *Proc Natl Acad Sci USA*. 2008;105:10513-10518.
14. Creemers EE, Tijsen AJ, Pinto YM. Circulating microRNAs: novel biomarkers and extracellular communicators in cardiovascular disease? *Circ Res*. 2012;110:483-495.
15. Leng Q, Wang Y, Jiang F. A Direct Plasma miRNA Assay for Early Detection and Histological Classification of Lung Cancer. *Transl Oncol*. 2018;11:883-889.
16. Chen TH, Lee C, Chiu CT, et al. Circulating microRNA-196a is an early gastric cancer biomarker. *Oncotarget*. 2018;9:10317-10323.
17. Moshiri F, Salvi A, Gramantieri L, et al. Circulating miR-106b-3p, miR-101-3p and miR-1246 as diagnostic biomarkers of hepatocellular carcinoma. *Oncotarget*. 2018;9:15350-15364.
18. Zhao K, Cheng J, Chen B, Liu Q, Xu D, Zhang Y. Circulating microRNA-34 family low expression correlates with poor prognosis in patients with non-small cell lung cancer. *J Thorac Dis*. 2017;9:3735-3746.
19. Moretti F, D'Antona P, Finardi E, et al. Systematic review and critique of circulating miRNAs as biomarkers of stage I-II non-small cell lung cancer. *Oncotarget*. 2017;8:94980-94996.
20. Zhou Q, Zhu Y, Wei X, et al. MiR-590-5p inhibits colorectal cancer angiogenesis and metastasis by regulating nuclear factor 90/vascular endothelial growth factor A axis. *Cell Death Dis*. 2016;7:e2413.
21. Ou C, Sun Z, Li X, et al. MiR-590-5p, a density-sensitive microRNA, inhibits tumorigenesis by targeting YAP1 in colorectal cancer. *Cancer Lett*. 2017;399:53-63.
22. Kim CW, Oh ET, Kim JM, et al. Hypoxia-induced microRNA-590-5p promotes colorectal cancer progression by modulating matrix metalloproteinase activity. *Cancer Lett*. 2018;416:31-41.
23. Jiang X, Xiang G, Wang Y, et al. MicroRNA-590-5p regulates proliferation and invasion in human hepatocellular carcinoma cells by targeting TGF-beta RII. *Mol Cells*. 2012;33:545-551.
24. Chen M, Wu L, Tu J, et al. miR-590-5p suppresses hepatocellular carcinoma chemoresistance by targeting YAP1 expression. *EBioMedicine*. 2018;35:142-154.
25. Shan X, Miao Y, Fan R, et al. MiR-590-5P inhibits growth of HepG2 cells via decrease of S100A10 expression and inhibition of the Wnt pathway. *Int J Mol Sci*. 2013;14:8556-8569.
26. Zhou L, Zhao LC, Jiang N, et al. MicroRNA miR-590-5p inhibits breast cancer cell stemness and metastasis by targeting SOX2. *Eur Rev Med Pharmacol Sci*. 2017;21:87-94.
27. Gao J, Yu SR, Yuan Y, et al. MicroRNA-590-5p functions as a tumor suppressor in breast cancer conferring inhibitory effects on cell migration, invasion, and epithelial-mesenchymal transition by down-regulating the Wnt-beta-catenin signaling pathway. *J Cell Physiol*. 2019;234:1827-1841.
28. Chu Y, Ouyang Y, Wang F, et al. MicroRNA-590 promotes cervical cancer cell growth and invasion by targeting CHL1. *J Cell Biochem*. 2014;115:847-853.
29. Yang X, Wu X. miRNA expression profile of vulvar squamous cell carcinoma and identification of the oncogenic role of miR-590-5p. *Oncol Rep*. 2016;35:398-408.
30. Xiao X, Tang C, Xiao S, Fu C, Yu P. Enhancement of proliferation and invasion by MicroRNA-590-5p via targeting PBRM1 in clear cell renal carcinoma cells. *Oncol Res*. 2013;20:537-544.
31. Wang L, Wei WQ, Wu ZY, Wang GC. MicroRNA-590-5p regulates cell viability, apoptosis, migration and invasion of renal cell carcinoma cell lines through targeting ARHGAP24. *Mol BioSyst*. 2017;13:2564-2573.
32. Shen B, Yu S, Zhang Y, et al. miR-590-5p regulates gastric cancer cell growth and chemosensitivity through RECK and the AKT/ERK pathway. *OncoTargets Ther*. 2016;9:6009-6019.
33. Zhang J, Zhou Y, Huang T, et al. FGF18, a prominent player in FGF signaling, promotes gastric tumorigenesis through autocrine manner and is negatively regulated by miR-590-5p. *Oncogene*. 2019;38:33-46.

34. Guo W, Zhang Y, Zhang Y, et al. Decreased expression of miR-204 in plasma is associated with a poor prognosis in patients with non-small cell lung cancer. *Int J Mol Med*. 2015;36:1720-1726.
35. Dinh TK, Fendler W, Chalubinska-Fendler J, et al. Circulating miR-29a and miR-150 correlate with delivered dose during thoracic radiation therapy for non-small cell lung cancer. *Radiation Oncol*. 2016;11:61.
36. Schmittgen TD, Livak KJ. Analyzing real-time PCR data by the comparative C(T) method. *Nat Protoc*. 2008;3:1101-1108.
37. Dzinic SH, Mahdi Z, Bernardo MM, et al. Maspin differential expression patterns as a potential marker for targeted screening of esophageal adenocarcinoma/gastroesophageal junction adenocarcinoma. *PLoS ONE*. 2019;14:e0215089.
38. Cappuzzo F, Hirsch FR, Rossi E, et al. Epidermal growth factor receptor gene and protein and gefitinib sensitivity in non-small-cell lung cancer. *J Natl Cancer Inst*. 2005;97:643-655.
39. Xu BB, Gu ZF, Ma M, Wang JY, Wang HN. MicroRNA-590-5p suppresses the proliferation and invasion of non-small cell lung cancer by regulating GAB1. *Eur Rev Med Pharmacol Sci*. 2018;22:5954-5963.
40. Slattery ML, Pellatt AJ, Lee FY, et al. Infrequently expressed miRNAs influence survival after diagnosis with colorectal cancer. *Oncotarget*. 2017;8:83845-83859.
41. Murria Estal R, Palanca Suela S, de Juan Jimenez I, et al. Relationship of immunohistochemistry, copy number aberrations and epigenetic disorders with BRCAness pattern in hereditary and sporadic breast cancer. *Fam Cancer*. 2016;15:193-200.
42. Zhang L, Li J, Wang Q, et al. The relationship between microRNAs and the STAT3-related signaling pathway in cancer. *Tumour Biol*. 2017;39:1010428317719869.
43. Yu Y, Zhao Q, He XP, Wang Z, Liu XY, Zhang ZP. Signal transducer and activator of transcription 3 overexpression promotes lymph node micrometastasis in early-stage non-small cell lung cancer. *Thoracic Cancer*. 2018;9:516-522.
44. Ai T, Wang Z, Zhang M, et al. Expression and prognostic relevance of STAT3 and cyclin D1 in non-small cell lung cancer. *Int J Biol Marker*. 2012;27:e132-e138.
45. Li X, Yu Z, Li Y, et al. The tumor suppressor miR-124 inhibits cell proliferation by targeting STAT3 and functions as a prognostic marker for postoperative NSCLC patients. *Int J Oncol*. 2015;46:798-808.
46. Galoczova M, Coates P, Vojtesek B. STAT3, stem cells, cancer stem cells and p63. *Cell Mol Biol Lett*. 2018;23:12.
47. Decker T, Kovarik P. Serine phosphorylation of STATs. *Oncogene*. 2000;19:2628-2637.
48. Hazan-Halevy I, Harris D, Liu Z, et al. STAT3 is constitutively phosphorylated on serine 727 residues, binds DNA, and activates transcription in CLL cells. *Blood*. 2010;115:2852-2863.
49. Carpenter RL, Lo HW. STAT3 Target Genes Relevant to Human Cancers. *Cancers*. 2014;6:897-925.
50. Lamouille S, Xu J, Derynck R. Molecular mechanisms of epithelial-mesenchymal transition. *Nat Rev Mol Cell Biol*. 2014;15:178-196.
51. Yuan J, Zhang F, Niu R. Multiple regulation pathways and pivotal biological functions of STAT3 in cancer. *Sci Rep*. 2015;5:17663.
52. Wang Y, Wu C, Zhang C, et al. TGF-beta-induced STAT3 overexpression promotes human head and neck squamous cell carcinoma invasion and metastasis through malat1/miR-30a interactions. *Cancer Lett*. 2018;436:52-62.
53. Huang Q, Han J, Fan J, et al. IL-17 induces EMT via Stat3 in lung adenocarcinoma. *Am J Cancer Res*. 2016;6:440-451.

How to cite this article: Khandelwal A, Seam RK, Gupta M, et al. Circulating microRNA-590-5p functions as a liquid biopsy marker in non-small cell lung cancer. *Cancer Sci*. 2020;111:826–839. https://doi.org/10.1111/cas.14199